Measurement of Erosion Rate by Absorption Spectroscopy in a Hall Thruster

Yamamoto, Naoji
Department of Advanced Energy Engineering Science, Kyushu University

Yokota, Shigeru
Department of Aeronautics and Astronautics, The University of Tokyo

Matsui, Makoto
Department of Advanced Energy, The University of Tokyo

Komurasaki, Kimiya
Department of Advanced Energy, The University of Tokyo

他

出版情報：Review of Scientific Instruments. 76 (8), pp.083111-083111, 2005-08. American Institute of Physics
バージョン：

Measurement of erosion rate by absorption spectroscopy in a Hall thruster

Naoji Yamamoto
Department of Advanced Energy Engineering Science, Kyushu University, 6-1 Kasuga-kouen, Kasuga, Fukuoka 816-8580, Japan

Shigeru Yokota
Department of Aeronautics and Astronautics, The University of Tokyo, Hongo 7-3-1, Bunkyo-ku, Tokyo 113-8656, Japan

Makoto Matsui and Kimiya Komurasaki
Department of Advanced Energy, The University of Tokyo, Kashiwanoha 5-1-5, Kashiwa, Chiba 277-8562, Japan

Yoshihiro Arakawa
Department of Aeronautics and Astronautics, The University of Tokyo, Hongo 7-3-1, Bunkyo-ku, Tokyo 113-8656, Japan

(Received 28 April 2005; accepted 16 June 2005; published online 3 August 2005)

The erosion rate of a Hall thruster was estimated with the objective of building a real-time erosion rate monitoring system using a 1 kW class anode layer type Hall thruster. This system aids the understanding of the tradeoff between lifetime and performance. To estimate the flux of the sputtered wall material, the number density of the sputtered iron was measured by laser absorption spectroscopy using an absorption line from ground atomic iron at 371.9935 nm. An ultraviolet $Al_xIn_yGa_{(1-x-y)}N$ diode laser was used as the probe. The estimated number density of iron was 1.1×10^{16} m^{-3}, which is reasonable when compared with that measured by duration erosion tests. The relation between estimated erosion rate and magnetic flux density also agreed with that measured by duration erosion tests. © *2005 American Institute of Physics.*
[DOI: 10.1063/1.2001630]

I. INTRODUCTION

Hall thrusters show considerable promise for satellite station keeping and orbit transfer applications[1,2] since they offer an attractive combination of high thrust efficiency, exceeding 50%, with a specific impulse range of 1000–3000 s and a higher ion beam density than ion thrusters. This is because Hall thrusters are not space charge limited.[3]

Several types of Hall thrusters are available, but they can be categorized into two general groups: namely, the anode layer type and the magnetic layer type.[4,5] One of the former type is the thruster with anode layer (TAL), which has been developed in Russia.[6,7] This thruster has a narrow acceleration zone for reducing the loss of ions and electrons due to collisions with the walls.[8,9] It has a conducting wall maintained at the cathode potential, and its acceleration channel length is shorter than its channel width.[10] The electron temperature of this type is higher than that of the other because there are no electron energy losses to the cathode potential wall.[5] The wall, or guard ring, protects the magnetic poles from ion bombardment. It is made of highly resistive materials against sputtering ions, such as pyrolitic graphite or stainless steel.[11] The short acceleration length and the highly resistive material will give the thruster the potential to have a longer lifetime than that which has been displayed by stationary plasma thrusters (SPTs).[9]

Lifetime is one of the most significant performance criteria for electric propulsion systems. There have been many studies on the lifetime of Hall thrusters, including endurance tests[12,13] and erosion measurements.[10,14] These studies show that the erosion of the acceleration channel wall is the main factor limiting the lifetime of the Hall thruster and that the erosion depends on operating condition, magnetic field configuration, wall material, anode configuration, and channel geometry. Understanding this dependence is essential for the practical application of Hall thrusters. It is not, however, practicable to validate the lifetime at each condition by means of typical wear tests because of the huge costs in time and money. Therefore, the measurement of the erosion rate by Laser Absorption Spectroscopy[15,16] is proposed. LAS has many advantages: (i) it could provide real-time monitoring of the erosion rate, (ii) it is a nonintrusive optical method for measuring the properties of plasmas, and (iii) it does not require absolute calibration, though a calibrated light source or a density reference cell is used in laser-induced fluorescence or emission spectroscopy,[17,18] since the number density of the absorbing atom can be deduced from the absorption profile of atomic lines in LAS. In addition, using an ultraviolet diode laser, it can measure the number density of the ground state of Fe directly without a large, expensive laser.

The purpose of this study is to validate this measurement technique in order to build a system for the real-time measurement of erosion rate by laser absorption spectroscopy. The anode layer type Hall thruster was used because the

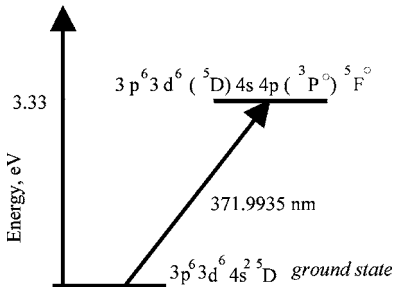

FIG. 1. Grotrian diagram of Fe I.

relation between thruster design and lifetime is not yet understood. This study contributes to the understanding of the tradeoff between lifetime and performance.

II. LASER ABSORPTION SPECTROSCOPY

The number density of sputtered iron from thruster acceleration walls was measured, since stainless steel is generally used for the acceleration channels of anode layer type Hall thrusters. Though stainless steel consists of Fe, Cr, and Ni, among other factors, the ratio of sputtered iron to eroded products is assumed to be equal to the chemical composition of it. The number density of Fe is estimated using the absorption line from ground state, as shown in Fig. 1.

The number density of the ground state n_g is related to the integrated absorption coefficient K as

$$K = \int_{-\infty}^{\infty} k_\nu \, d\nu = \frac{c^2}{\nu^2} \frac{1}{8\pi} \frac{g_e}{g_g} A_{eg} n_g \left[1 - \exp\left(- \frac{\Delta E_{ge}}{kT_{ex}} \right) \right]. \quad (1)$$

Here, k_ν is the absorption coefficient at the frequency of ν, g is the statistical weight, the subscripts $_g$ and $_e$ denote the ground and excited states, ΔE is the energy gap, and A is the Einstein coefficient. At 371.9935 nm, $g_g=9$, $g_e=11$, $\Delta E_{ge}=3.33$ eV, and $A_{eg}=1.62\times10^7$ s^{-1}.[19]

III. EXPERIMENTAL EQUIPMENT

A. Thruster

Figure 2 shows a cross section of a 1 kW class anode layer type Hall thruster.[20] The inner and outer diameter of the acceleration channel are 48 mm and 62 mm, respectively. The outer diameter, ϕ_{out}, can be changed to 72 mm. A solenoidal coil at the center of the thruster creates a radial magnetic field in the acceleration channel. No outer coil is used, so that the magnetic field distribution is kept uniform along the azimuthal direction. The magnetic field distribution along the channel median is almost uniform in the short acceleration channel. Magnetic flux density is maximized on the inner wall and decreases with radius, since the magnetic flux is constant. Guard rings are made of stainless steel (SUS304). The separation between the guard ring and the anode is 1 mm. The thruster has a hollow annular anode, which consists of two cylindrical rings, with a propellant gas fed through them. The width of the hollow anode is 3 mm ($\phi_{out}=62$ mm) or 8 mm ($\phi_{out}=72$ mm), and the gap between the tip of the anode and the exit of the acceleration channel is fixed at 3 mm. The thruster operating conditions and facility backpressure are shown in Table I.

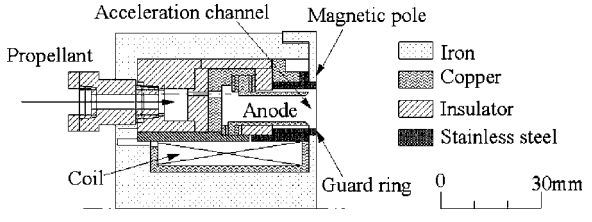

FIG. 2. Cross section of the anode layer type Hall thruster developed at the University of Tokyo.

TABLE I. Thruster operating conditions.

Mass flow rate anode	Cathode	Facility backpressure
2.72 mg/s (±0.05 mg/s)	0.27 mg/s (±0.02 mg/s)	5.3×10^{-3} Pa
4.08 mg/s (±0.05 mg/s)	0.27 mg/s (±0.02 mg/s)	7.5×10^{-3} Pa

High-purity (99.999% pure) xenon gas was used as the propellant. Thermal mass flow controllers (Kofloc, 3610) are used. A hollow cathode (Ion Tech HC-252) was used as the electron source.

B. Vacuum chamber

A vacuum chamber of 2 m diameter by 3 m length was used in the experiments. The pumping system consists of a diffusion pump, a mechanical booster pump, and two rotary pumps. The chamber was made of 316 stainless steel. The effect of iron eroded from the chamber wall can be neglected. Since the thruster is set at far field from the chamber wall, eroded atoms that come to the measurement region from the chamber wall are 1% less than that from the thruster.

C. Experimental apparatus and conditions

A schematic of the measurement system is shown in Fig. 3. An ultraviolet diode laser $Al_xIn_yGa_{(1-x-y)}N$ (Nichia, NDHU200APAE2)[21] was used as a probe. The frequency was swept by current modulation, at a modulation width of 8 GHz. An optical chopper (Stanford Research Systems, SR540) and a lock-in amplifier (Stanford Research Systems, SR510) were used for elimination of plasma emission. The laser beam was divided in two by a beam splitter. One beam was detected by an optical spectrum analyzer (Advantest, Q8347) for the measurement of the frequency. Its resolution was 1 GHz. The other beam was used as a probe, passing in front of the thruster and being detected by a photodetector (Thorlabs, DET110/M). The laser beam was passed as shown in Fig. 4 for the enhancement of sensitivity.

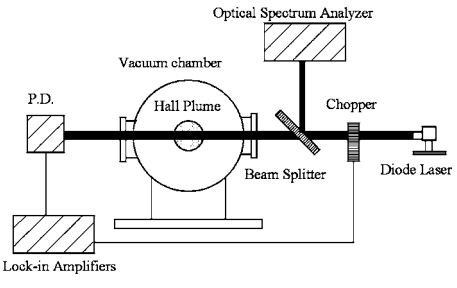

FIG. 3. Schematic of measurement system.

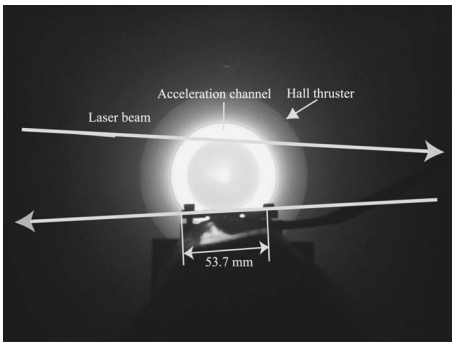

FIG. 4. Photograph of Hall thruster operation.

A monochromator (Hamamatsu Photonics, PMA-50) was used for the simultaneous measurement of the electron excitation temperature. The grating was 2400 grooves/mm and the dispersion was 0.02 nm/ch. The wavelength resolution was 0.05 nm.

IV. RESULTS AND DISCUSSION

There are spectra that are not used for the measurement since this laser diode has multiple longitudinal modes, as shown in Fig. 5. The linewidth of the laser was less than 1 GHz, which is the maximum resolution of the optical spectrum analyzer. Although lasers with multiple longitudinal modes are not adequate for laser absorption spectroscopy, there is no ultraviolet laser diode with a single longitudinal mode. In addition, there was, at the time of the experiment, no available ultraviolet laser diode with an external cavity, because of the difficulty of applying antireflective coating. Thus, this laser was used with compensation, that is, the intensity of the absorption line was estimated by normalization of the laser intensity from the spectral distribution, since the photodetector detects the intensity of all the spectra. Figure 6 shows the ratio of the target spectrum to all spectra. It was almost constant, 0.14, during frequency modulation.

Figure 7 shows the compensated absorption profile for operational conditions of $\phi_{\text{out}}=62$ mm, $V_{\text{d}}=400$ V, $\dot{m}=2.72$ mg/s, and $B_r=0.034$ T. Here, ϕ_{out} is the outer diameter of the acceleration channel, V_{d} is the discharge voltage, $\dot{m}$ is the mass flow rate, and B_r is the magnetic flux density at the channel median. The electron excitation temperature was 0.35 eV based on the Boltzmann plot for Fe I, as shown in Fig. 8. The transition data for this measurement are shown in Table II, as quoted from the NIST database.[19] Thus, stimulated emission can be neglected, since $\Delta E_{ge}/kT_{\text{ex}}=9.43>1$.

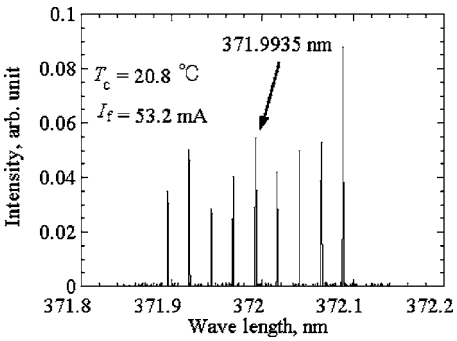

FIG. 5. Spectrum of ultraviolet laser diode at $I_f=53.2$ mA.

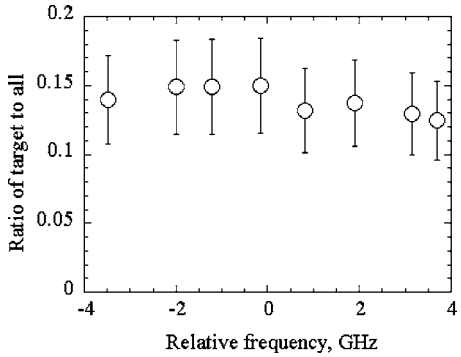

FIG. 6. Ratio of target spectrum to all the spectra.

The optical path length is assumed to be the crossing distance of the laser beam in front of the acceleration channel, or 0.078 m. The number density of Fe was estimated to be 1.1×10^{16} m^{-3}, since the number density of the ground state of Fe I would be almost equal to that of Fe as a result of the low electron excitation temperature.

The erosion rate for these conditions was estimated to be about 0.06 g/h from the experimental results of the wear lifetime test of this thruster.[22] If we compensate for differences in operating conditions, discharge voltage, and the sputter yield of copper and stainless steel, we arrive at 0.28 g/h. Considering that SUS304 consists of 74% Fe, and half of the sputtered iron is assumed to leave from the thruster, the sputtering rate was estimated as

$$\dot{m}_{\text{SUS}}=2\times\frac{1}{0.74}SM_{\text{Fe}}N_{\text{Fe}}V_{\text{Fe}}=0.06\ \text{g/h}. \tag{2}$$

This erosion rate is equal to 0.06 g/h, thus the average velocity of the Fe atoms, V_{Fe} was estimated as

$$V_{\text{Fe}}=\frac{\dot{m}_{\text{SUS}}}{SM_{\text{Fe}}N_{\text{Fe}}}\times\frac{0.74}{2}=2.6\times10^{3}\ \text{m/s}. \tag{3}$$

This value is reasonable, since the sputtered atoms can be assumed to have about 1% of the energy of a sputtering ion,[23] or

$$V_{\text{Fe}}=\sqrt{\frac{2eE_{\text{Xe}}\times0.01}{M_{\text{Fe}}}}\approx3.5\times10^{3}\ \text{m/s}. \tag{4}$$

Next, the dependence of the erosion rate on operational conditions was investigated. Unfortunately, the measurement absorption rate is too small to discriminate among various conditions. Thus, the probe beam was not detected by the

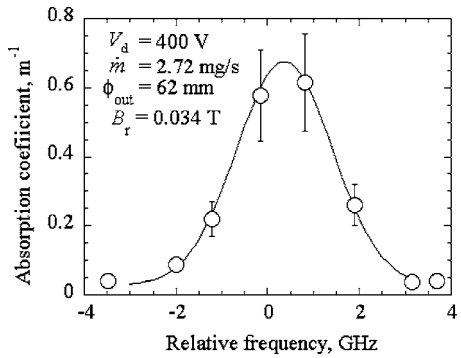

FIG. 7. Absorption profile of target spectrum.

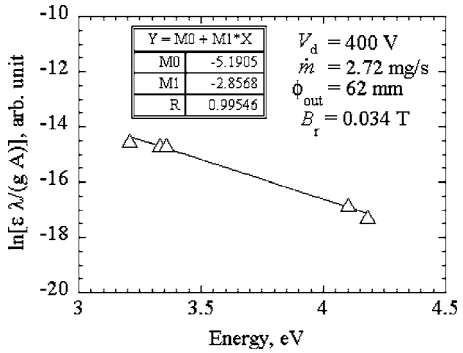

FIG. 8. Boltzmann plot for Fe I.

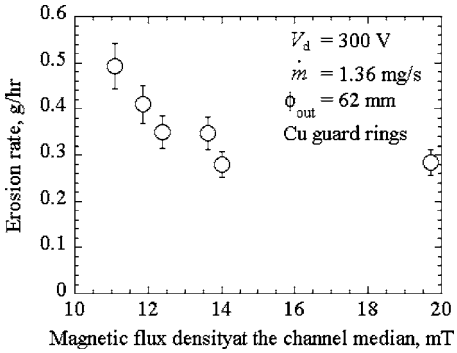

FIG. 10. Relation between erosion rate and magnetic flux density.

TABLE II. Transition data for Fe I.

Wavelength (nm)	E_k (eV)	A_{ki} 10^8 s^{-1}	g_i-g_k
371.99	3.33	0.16	9–11
373.49	4.18	0.9	11–11
373.71	3.36	0.14	7–9
382.04	4.1	0.67	11–9
385.99	3.21	0.1	9–9

photodetector but by the optical spectrum analyzer. This can detect only the intensity of the target spectra, and its resolution is less than that of the photodetector.

The outer diameter of the thruster was changed to 72 mm for the enhancement of sensitivity. That is, in order to increase the absorption rate, the optical path length was increased from 0.078 to 0.107 m. Figure 9 shows the relation between the estimated erosion rate of the guard rings and the magnetic flux density. The average velocity of sputtered iron was estimated as in Eq. (4). The erosion rate decreased with magnetic flux density, though beyond the critical magnetic flux density, it increased slightly with magnetic flux density. This result agreed with that of duration erosion tests.[22] That is, the erosion rate by means of duration erosion tests also decreased with magnetic flux density, and beyond the critical magnetic flux density, it increased slightly, as shown in Fig. 10.

The above results prove the possibility of a nonintrusive real-time erosion rate monitoring system for electric propulsion. Though this system is not strictly real-time erosion rate monitoring, it will enable us to understand the dependence of lifetime on operating conditions or thruster design without the need for lengthy tests.

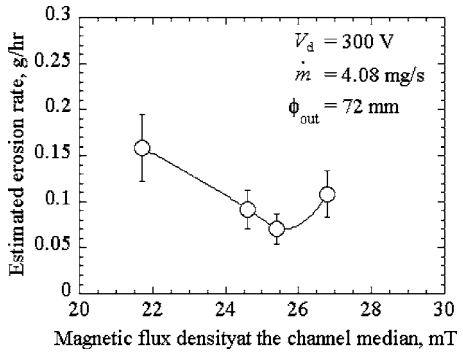

FIG. 9. Relation between erosion rate and magnetic flux density.

ACKNOWLEDGMENT

The present work was supported by a Grant-in-Aid for Scientific Research (S), No. 16106012, sponsored by the Ministry of Education, Culture, Sports, Science and Technology, Japan.

[1] G. Saccoccia, "Introduction to the European Activities in Electric Propulsion," IEPC Paper 03-341 (2003).
[2] J. Blandino, "The Year in Review: Electric Propulsion" Aerosp. Am. **12**, 60 (2003).
[3] V. Kim, J. Propul. Power **14**, 736 (1998).
[4] H. R. Kaufman, AIAA J. **23**, 78 (1985).
[5] E. Y. Choueiri, Phys. Plasmas **8**, 5025 (2001).
[6] A. V. Zharinov and Yu. S. Popov, Sov. Phys. Tech. Phys. **12**, 208 (1967).
[7] C. E. Garner, J. R. Brophy, J. E. Polk, A. V. Semenkin, V. I. Garlusha, S. O. Tverdokhlebov, and C. Marrese, AIAA Paper 94-3010 (1994).
[8] Yu. S. Popov and Yu. M. Zolotaikin, Sov. J. Plasma Phys. **3**, 210 (1977).
[9] V. V. Zhurin, H. R. Kaufman, and R. S. Robinson, Plasma Sources Sci. Technol. **8**, R1 (1999).
[10] A. V. Semenkin, IEPC Paper 93-231 (1993).
[11] A. E. Solodukhin and A. V. Semenkin, IEPC Paper 2003-0204 (2003).
[12] C. E. Garner, J. R. Brophy, J. E. Polk, and L. C. Pless, AIAA Paper 95-2667 (1995).
[13] A. V. Semenkin, A. Kochergin, A. Rusakov, V. Bulaev, J. Yuen, J. Shoji, C. Garner, and D. Manzella, AIAA Paper 99-2279 (1999).
[14] D. T. Jacobson, AIAA Paper 02-4257 (2002).
[15] M. P. Arroyo, S. Langlogis, and R. K. Hanson, Appl. Opt. **33**, 3296 (1994).
[16] F. Y. Zhang, K. Komurasaki, T. Iida, and T. Fujiwara, Appl. Opt. **38**, 1814 (1999).
[17] G. J. Williams, T. B. Smith, F. S. Gulczinski, and A. D. Gallimore, J. Propul. Power **18**, 489 (2002).
[18] R. J. Cedolin, W. A. Hargus, Jr., P. V. Storm, R. K. Hanson, and M. A. Cappelli, Appl. Phys. B: Lasers Opt. **65**, 459 (1997).
[19] http://www.physics.nist.gov/PhysRefData/ASD/lines_form.html
[20] N. Yamamoto, T. Nakagawa, K. Komurasaki, and Y. Arakawa, J. Jpn. Soc. Aeronaut. Space Sci. **51**, 492 (2003) (in Japanese).
[21] S. Nagahama, T. Yanamoto, M. Sano, and T. Mukai, J. Jpn. Soc. Aeronaut. Space Sci. **41**, 5 (2002).
[22] N. Yamamoto, T. Nakagawa, K. Komurasaki, and Y. Arakawa, *Proceedings of the 23rd International Symposium on Space Technology and Science* (2002), p. 319.
[23] B. N. Chapman, *Glow Discharge Processes: Sputtering and Plasma Etching* (Wiley, New York, 1980).